

Numerical Simulation and Experimental Validation of the Boundary Layer Generated by a Turbulent Flow on a Hydraulically Smooth Bed

¹D. Tcheukam-Toko, ²L. Kongue, ¹C.A. Koueni-Toko, ¹R. Mouangue and ³M. Belorgey

¹Department of Energetic Engineering, University Institute of Technology (IUT),

²Department of Physics, Faculty of Science, University of Ngaoundere,

P.O. Box 454, Ngaoundere, Cameroon

³M2C-Fluid Mechanic Group, UMR-CNRS 6143, University of Caen, F-14000 Caen, France

Abstract: This study is for incompressible flow at constant viscosity. It consists of a numerical simulation and an experimental validation for a boundary layer generated by a turbulent flow on a hydraulically smooth bed. The device considered here is a hydraulically smooth plate of length 15 m and of 0.27 m high. The study treats the influence of the reynolds number on the thickness of the boundary layer, on the turbulent of friction and on the longitudinal velocity into the boundary layer. This problem was approached by using gambit calculation code to generate the mesh. These one adopted here is the structured type which is very narrow at the bottom level of the plate. Researchers used also fluent code to solve the general equations of the boundary layer. The system of equations being the open type, we are forced here to use the k-ε Standard Turbulent Model. The results obtained shows that there is a good concordance with the experimental results and thus Validates Model.

Key words: Boundary layer, smooth bed, numerical validation, turbulent flow, plate, mesh

INTRODUCTION

The turbulent flows are present in a large number of scientific engineering applications such as energy, environment, transport and biotechnology. These flows are unsteady often coupled and generates other physics phenomenon such as the boundary layer.

We are going to study numerically the influence of the turbulent incompressible flow on a hydraulically smooth bed. Descamps shows that in the boundary layer, there are two zones: the internal and the external zones. In these two zones we have under layers: under viscous layer, the pad region, the recovery region and the wake region. According to the Classical Model of Van Driest (1956) and of Cebeci and Smith (1974), a turbulent boundary layer on the plate does not only have a strong velocity gradient closed to the wall but has equally two zones: a viscous zone and a logarithmic zone which are each characterised by a velocity law. Tcheukam-Toko proposes a mixing length model while taking into account the different natures of the viscous and turbulent zones.

The aim of this study is to determine in function of the initial reynolds number flow, the velocity and the evolution of the velocity field along the walls the thickness of the boundary layer and the turbulent friction. This is later compared to the experimental measurement of

Tcheukam-Toko. In order to better this study, it will be presented mathematical models to be used, experimental devices and numerical results that will be discussed and concluded.

MATERIALS AND METHODS

Mathematical models used: The continuity equation is given by the Eq. 1:

$$\frac{\partial \rho}{\partial t} + \text{div}(\rho \vec{V}) = 0 \quad (1)$$

The conservation equations of the average quantity of movement of Navier-Stokes known by the name RANS are for compressible fluid and Newtonian given by the equation:

$$\frac{\partial}{\partial t}(\rho u_i) + \underbrace{\frac{\partial}{\partial x_j}(\rho u_i u_j)}_{\text{Convective transport}} = - \underbrace{\frac{\partial P}{\partial x_i}}_{\text{Forces due to pressures}} + \underbrace{\frac{\partial}{\partial x_j} \left[\mu \left(\frac{\partial u_i}{\partial x_j} + \frac{\partial u_j}{\partial x_i} - \frac{2}{3} \delta_{ij} \frac{\partial u_k}{\partial x_k} \right) \right]}_{\text{Viscosity forces}} + \underbrace{\frac{\partial}{\partial x_j} \left(-\overline{\rho u_i u_j} \right) + F_i}_{\text{Forces generated by turbulence}} \quad (2)$$

$-\rho \overline{u_i u_j}$ are the components of the Reynolds stress. Its expression is as given by the Boussinesq hypothesis:

$$-\rho \overline{u_i u_j} = \mu_t \left(\frac{\partial u_i}{\partial x_j} + \frac{\partial u_j}{\partial x_i} \right) - \frac{2}{3} \left(\rho k + \frac{\partial u_i}{\partial x_j} \right) \delta_{ij} \quad (3)$$

The k-ε turbulence models used by the Software FLUENT are:

- The k-ε Standard Model
- The k-ε RNG Model
- The k-ε Realisable Model

We are going to use the k-ε realisable model to carry out the calculations. Since, it was applied successfully for the simulation of an important variety of turbulent flow (boundary layer, circular conduit flow, open channel flow). This model combines the simplicity of mathematical formulation, the reality of turbulent transport phenomenon and economies in term of numerical calculations.

The transport equations for the k-ε standard model are: The transport equations of turbulent kinetic energy which is given by the equation:

$$\overline{u_j} \frac{\partial k}{\partial x_j} = C_\mu \frac{k^2}{\varepsilon} \left(\frac{\partial \overline{u_i}}{\partial x_j} + \frac{\partial \overline{u_j}}{\partial x_i} \right) \frac{\partial \overline{u_i}}{\partial x_j} + \frac{\partial}{\partial x_j} \left(\frac{C_\mu k^2}{\sigma_k \varepsilon} \frac{\partial k}{\partial x_j} \right) - \varepsilon \quad (4)$$

Where:

- $\overline{u_j} \frac{\partial k}{\partial x_j}$ = The variation of the turbulent kinetic energy
- $C_\mu \frac{k^2}{\varepsilon} \left(\frac{\partial \overline{u_i}}{\partial x_j} + \frac{\partial \overline{u_j}}{\partial x_i} \right) \frac{\partial \overline{u_i}}{\partial x_j}$ = The production of turbulent kinetic energy
- $\frac{\partial}{\partial x_j} \left[\frac{C_\mu k^2}{\sigma_k \varepsilon} \left(\frac{\partial k}{\partial x_j} \right) \right]$ = The term of diffusion
- ε = The dissipation

The transport equation of the dissipation rate of turbulent kinetic energy which is given by the equation:

$$\overline{u_j} \frac{\partial \varepsilon}{\partial x_j} = C_{\varepsilon 1} C_\mu k \left(\frac{\partial \overline{u_i}}{\partial x_j} + \frac{\partial \overline{u_j}}{\partial x_i} \right) \frac{\partial \overline{u_i}}{\partial x_j} + \frac{\partial}{\partial x_j} \left(\frac{C_\mu k^2}{\sigma_\varepsilon \varepsilon} \frac{\partial \varepsilon}{\partial x_j} \right) - C_{\varepsilon 2} \frac{\varepsilon^2}{k} \quad (5)$$

Where the turbulent viscosity is calculated from k-ε by using the relation Eq. 6:

$$\nu_t = \frac{C_\mu k^2}{\varepsilon} \quad (6)$$

The k-ε Model brings into intervention five constants which are shown in Table 1.

Table 1: Standard values of k-ε constant

C_μ	$C_{\varepsilon 1}$	$C_{\varepsilon 2}$	σ_ε	σ_k
0.09	1.44	1.92	1.3	1.0

Table 2: The grid detail

Grid sizes	Number of cells
1	1700
2	2375
3	3300

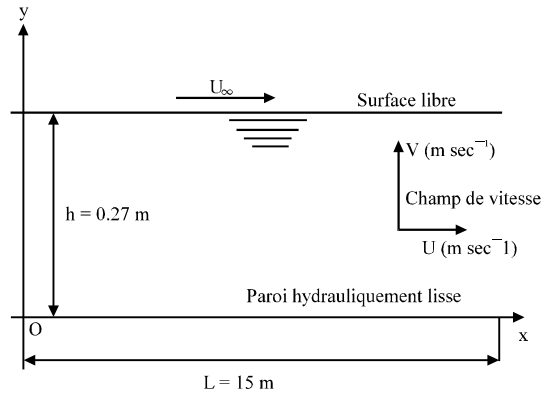


Fig. 1: Experimental device

Experimental device: Consider for this numerical study a boundary layer generated by a free surface permanent incompressible flow. The reference coordinates considered is shown in Fig. 1.

The domain of calculation is inspired from the experimental pattern of Tcheukam-Toko. This domain is a plate of length 15 m, the height of water is 0.27 m. The evaluation of the velocity profiles is determined by the longitudinal means velocities values of 0.027, 0.035, 0.042, 0.050 and 0.058 corresponding, respectively to the Reynolds numbers of 3660, 4150, 4500, 5000 and 5200. The Reynolds number is a dimensional number which is relative to the thickness of the boundary layer and is written by the relation:

$$Re = U_m \delta / \nu \quad (7)$$

In this study, the sign + indicates a standard size, $U^+ = U/U_{max}$; $X^+ = x/L$ and $Y^+ = y/\delta$. The water flows on the left plate towards the right at the temperature of 25°C.

Mesh and boundaries conditions: Three types of grids are being used to determine the behaviour of the solution to the problem composed in function of the grid size. The details of the mesh size are shown in Table 2.

The grid 1 is the biggest serving in the calibration of the calculation. The grid 2 and 3 gives the definitive results of the simulation.

In Fig. 2, it is seen that the solution of the velocity does not change in a significant manner ($\leq 5\%$) between the mesh sizes 2 and 3. The solution is thus independent of the mesh size. Researchers chosen the mesh size 2 since, it gives an optimal solution.

The grid is realised with the Gambit program. It is a regular grid type with quadrilateral cell forms. The calculation is optimised in shedding the mesh size close to the walls. The Fig. 3 represents the calculation domain of the mesh size. To have the boundaries conditions, we have imposed at the input of the calculation domain, the velocities conditions. The velocities values are identical to that of Tchekam-Toko and at the output domain, we have imposed the pressure conditions. On the walls, we have imposed a null velocity. The different boundaries conditions are shown in Fig. 4.

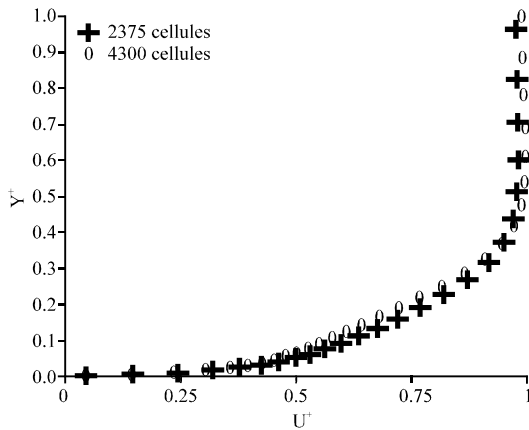


Fig. 2: Comparison of velocity profiles in function of the grid numbers

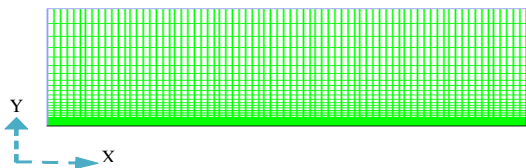


Fig. 3: Calculation domain of the mesh size 2

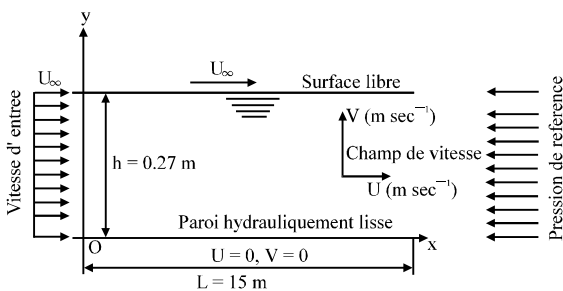


Fig. 4: Boundaries conditions

RESULTS AND DISCUSSION

The results of the numerical simulation made at full capacity, shows the influence of the flow initial velocity on the dynamic field along the plate. The Fig. 5 shows the velocity profiles along the plate in function of different Reynolds numbers. It is seen that for $Re = 3660$, the velocity attends 99% of the initial velocity at the position where $y = 5$ cm. This value of y at which the velocity attends 99% of its initial velocity increases progressively with the rise of reynolds numbers and for $Re = 4500$, we obtains $y = 7$ cm.

Figure 6 shows the evolution of the boundary layer along the hydraulically smooth walls for an initial velocity of 0.035 m sec^{-1} . From Fig. 6, it is seen that the thickness of the boundary layer is null at the stroke of the plate considered to be infinity thin. It rises afterwards constantly when the x -axis increases.

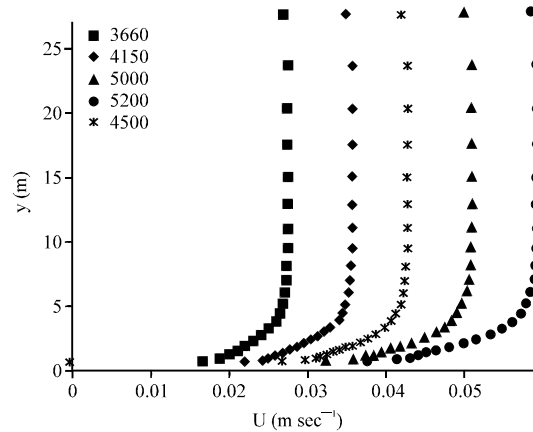


Fig. 5: Average velocity distributions for different positions of X

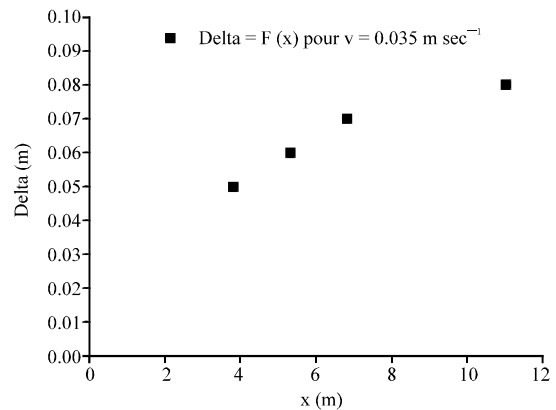


Fig. 6: Thickness of the boundary layer in function of the x for $U = 0.035 \text{ m sec}^{-1}$

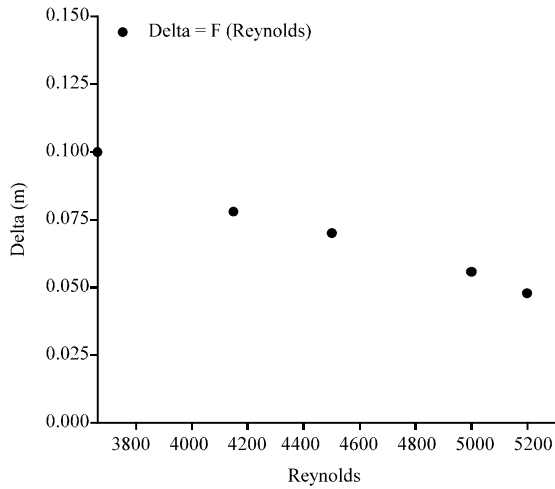


Fig. 7: Thickness of the boundary layer in function of the Reynolds number

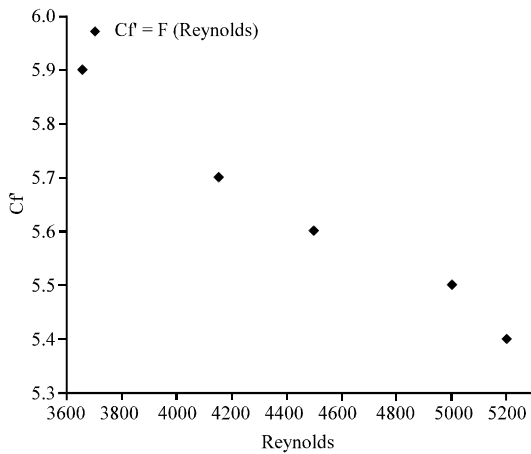


Fig. 8: Coefficient of turbulent friction in function of the Reynolds number

Figure 7 shows that the thickness of the boundary layer decreases with increase in the Reynolds number. Figure 8 shows the evolution of the turbulent friction coefficient in function of the Reynolds number. From Fig. 8, it is noted that the coefficient of turbulent friction decreases slightly with increase in the Reynolds number. This permit to confirm that the variation of the turbulent friction at the bottom is directly linked to the flow discharge variations.

$$Cf = \text{Coefficient de frottement} \times 100$$

Comparison of results: Figure 9-11 shows the velocity profiles obtained by numerical simulation and the experimental results of Tcheukam-Toko, for the different

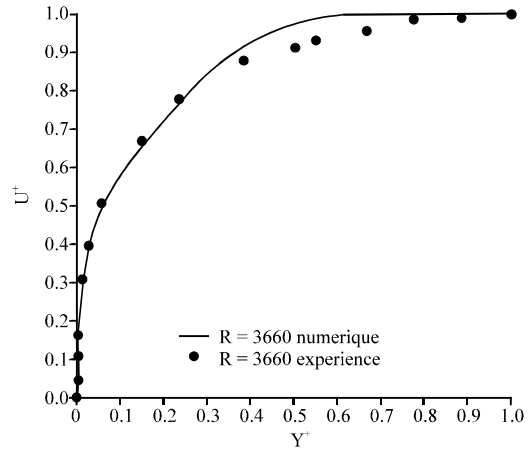


Fig. 9: Comparison of velocity profiles, for Re = 3660

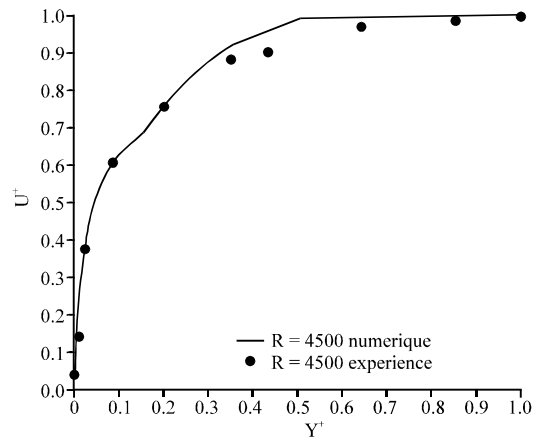


Fig. 10: Comparison of velocity profiles, for Re = 4150

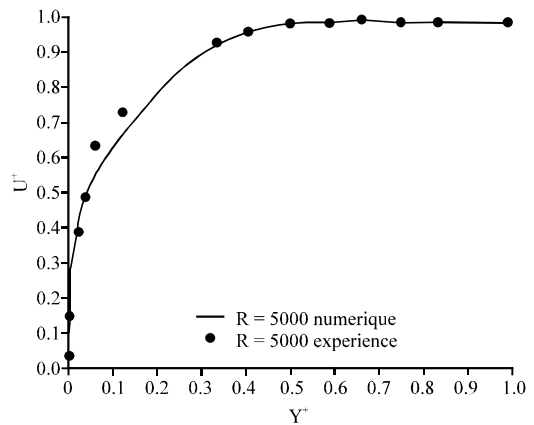


Fig. 11: Comparison of velocity profiles, for Re = 5000

values of Reynolds numbers: 3660, 4150, 4500 and 5000. We notice that the velocity profiles obtained by numerical simulation are at a good concordance with the experimental profiles.

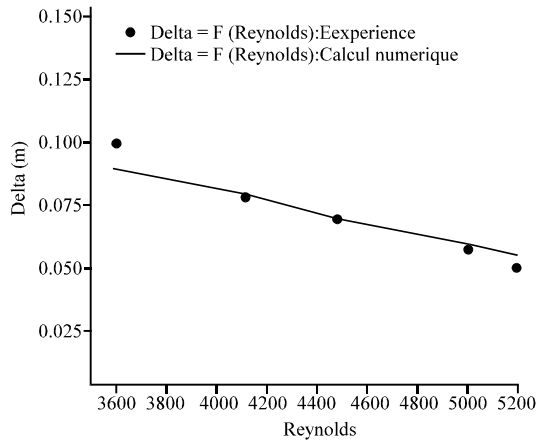


Fig. 12: Comparison of the boundary layer thicknesses

Figure 12 shows the comparison of thickness of the boundary layer obtained by numerical calculation and by experiments measurement. The researchers notice that these two results are in good accord.

CONCLUSION

As far as this research is concern, researchers notice that the velocity profile into the boundary layer increases with the Reynolds number mean while the turbulent friction and the thickness of the boundary layer decreases Murzyn and Belorgey (2002), Tcheukam-Toko *et al.* (2008). The comparison with the results of Tcheukam-Toko is satisfactory. These results made at full capacity, can be carried out in an unstable condition in order to better the representation of the flow. The velocity fluctuations can be also analysed to better apprehend the turbulence phenomenon in the boundary layer.

ACKNOWLEDGEMENT

The researchers acknowledge The University of Caen, France and The University of Ngaoundere, Cameroon.

NOMENCLATURE

- x = Longitudinal coordinat (m)
- y = Vertical coordinat (m)
- ν = Kinetic viscosity of water ($m^2 \text{ sec}^{-1}$)
- μ = Dynamic viscosity of water (Pa sec)
- ϵ = Dissipation ratio of the turbulent kinetic energy
- K = Turbulent kinetic energy ($J \text{ kg}^{-1}$)
- ρ = Density of liquid ($kg \text{ m}^{-3}$)
- Re = Reynolds number
- pr_t = Prandtl turbulent number
- + = No dimensional number (by H for length) and (by ΔT_{ref} for temperature difference)
- μ_t = Turbulent viscosity
- x = Relative to the longitudinal component
- y = Relative to vertical component

REFERENCES

- Cebeci, T. and A.M.O. Smith, 1974. Analysis of Turbulent Boundary Layer. Academic Press, New York, USA.
- Murzyn, F. and M. Belorgey, 2002. Turbulence structure in free-surface channel flows. Proceedings of the Hydraulic Measurements and Experimental Methods Conference, July 28, 2002, Estes Park, Colorado.
- Tcheukam-Toko, D., M. Belorgey and M. Movahedan, 2008. Study of turbulent friction in a gradually varied flow. Res. J. Applied Sci., 3: 465-470.
- Van Driest, E.R., 1956. Turbulence flow near a wall. J. Aeron. Sci., 23: 1007-1011.